

PSEUDO 3-D FULL-CORE CONJUGATE HEAT TRANSFER MODELING OF SODIUM FAST REACTORS

Rui Hu and Yiqi Yu

Nuclear Engineering Division, Argonne National Laboratory,
9700 S. Cass Avenue, Argonne IL 60439, USA
rhu@anl.gov, yyu@anl.gov

ABSTRACT

For efficient and accurate temperature predictions of sodium fast reactor structures, a 3-D full-core conjugate heat transfer modeling capability is developed for an advanced system analysis tool, SAM. The hexagon lattice core is modeled with 1-D parallel channels representing the subassembly flow, and 2-D duct walls and inter-assembly gaps. The six sides of the hexagon duct wall are modeled separately to account for different temperatures and heat transfer between inner assembly flow and each side of the duct wall. The Jacobian Free Newton Krylov (JFNK) solution method is applied to solve the fluid and solid field simultaneously in a fully coupled fashion. The 3-D full-core conjugate heat transfer modeling capability in SAM has been demonstrated by a verification test problem with 7 fuel assemblies in a hexagon lattice layout. Additionally, the simulation results are compared with RANS-based CFD simulations. Very good agreements have been achieved between the results of the two approaches.

KEYWORDS

conjugate heat transfer, pseudo-3D, sodium fast reactor, and system thermal-hydraulics

1. INTRODUCTION

One important design requirement for sodium-cooled fast reactors (SFR) is the knowledge of the temperature on the hexagonal ducts for a thermo-mechanical analysis. This is particularly important to ensure the passive safety of the reactor under the unprotected accident conditions if the reactor control system fails to function and the reactivity feedback from structural deformation such as core radial expansion is significant [1]. This information requires a good evaluation of the inter-assembly flow and heat transfer in this region. The physical phenomena are particularly complicated and require a reliable modeling of the whole core including the inter-assembly region.

Multiple levels of modeling are possible for the analysis of the whole core thermal hydraulic behavior, depending on the purpose of the calculation and the accuracy required. Generally, the 3D full core modeling using the computational fluid dynamics (CFD) approach is prohibitively expensive. Porous medium models have been applied to predict SFR duct wall temperatures, which is much less computationally expensive than conventional CFD simulations that explicitly represent the wire-wrap and fuel pin geometry [2]. However, even porous medium or subchannel description of each subassembly and the inter-assembly space is still too computationally expensive for quotidian analyses. System analysis is favorable to describe the global behavior of the whole core during transient situations.

In traditional reactor safety analysis, the reactor core is modeled with several 1D parallel channels to take into account the main different core regions, with a possible by-pass channel to simulate amassed flow

rate in the inter-assembly zone [3]. However, it is very cumbersome to obtain the detailed temperature predictions of inter-assembly gaps and duct walls, which requires a full-core one-to-one representation of fuel assemblies and inter-assembly gaps.

For efficient and accurate temperature predictions of SFR structures, a 3-D full-core conjugate heat transfer modeling capability has been developed for an advanced system analysis tool, SAM, being developed at Argonne National Laboratory. The hexagon lattice core can be modeled with 1-D parallel channels representing the subassembly flow and 2-D duct walls and intra-assembly gaps, in one-to-one representation. Note that the 6 sides of the hexagon duct wall are modeled separately to account for different temperatures and heat transfer between inner assembly flow and each side of the duct wall. A core lattice model has been developed in SAM so that it can, based on very simple input descriptions, generate all the core channels and inter-assembly gaps, and build the connections among them.

The general overview of the SAM code can be found in Ref. [4]; and the in-depth discussion of the underlying physics models and numerical methods can be found in Ref. [5-6]. This paper firstly gives a brief overview of the SAM code, and then presents the conjugate heat transfer modeling method in SAM. Additionally, the 3-D full-core conjugate heat Transfer modeling capability is demonstrated by a verification test problem with 7 fuel assemblies in a hexagon lattice layout. The simulation results are compared with the RANS-based CFD simulation using the commercial CFD code STAR-CCM+ [7]. Good agreements have been achieved between the results of the two approaches.

2. OVERVIEW OF SAM THERMAL-HYDRAULICS MODEL

SAM is an advanced system analysis tool being developed at Argonne National Laboratory under the U.S. DOE's Nuclear Energy Advanced Modeling and Simulation (NEAMS) program. The code is aimed to solve the tightly-coupled physical phenomena including fission reaction, heat transfer, fluid dynamics, and thermal-mechanical response in the SFR structures, systems and components in a fully-coupled fashion but with reduced-order modeling approaches to facilitate rapid turn-around for design and safety optimization studies. As a new code development, the initial effort focused on developing modeling and simulation capabilities of the heat transfer and single-phase fluid dynamics responses in the SFR systems.

SAM utilizes an object-oriented application framework (MOOSE [8]), the underlying meshing and finite-element library (libMesh [9]), and linear and non-linear solvers (PETSc [10]) to leverage the available advanced software environments and numerical methods. The physics modeling and mesh generation of individual reactor components are encapsulated as component classes in SAM along with some component specific models. A set of components has been developed based on the finite element models (for fluid flow and heat transfer), and the system simulation capabilities of general thermal-hydraulics systems have been demonstrated [11].

Fluid dynamics is the main physical model of the SAM code. SAM employs a one-dimensional transient model for single-phase incompressible but thermally expandable flow. The details of the single-phase flow model for incompressible thermally expandable flow can be found in Ref. [5]. The transport equations for one-dimensional, single-phase flow can be described by the following set of partial differential equations. The mass, momentum, and energy conservation equations are closed by the equation of state for the fluid. After the simplifications, the set of governing equations can be written in the conservative form (Eq.-1).

$$\begin{aligned}
\frac{\partial \rho}{\partial t} + \frac{\partial(\rho u)}{\partial z} &= 0 \\
\frac{\partial(\rho u)}{\partial t} + \frac{\partial(\rho u u + p)}{\partial z} &= -\rho g - \frac{f}{D_e} \frac{\rho u |u|}{2} \\
\frac{\partial(\rho H)}{\partial t} + \frac{\partial(\rho u H)}{\partial z} &= q''' \\
p &= p(\rho, \rho u, \rho E) \text{ or } \rho = \rho(p, T)
\end{aligned} \tag{1}$$

In which f : the friction coefficient; D_e : equivalent hydraulic diameter. When considering the convection heat flux from solid surface q_s'' , $q''' = q_s'' P_h / A_c$, where P_h and A_c respectively denote heated perimeter and cross-sectional area of the coolant channel.

Heat structures model the heat conduction inside the solids and permit the modeling of heat transfer at the interfaces between solid and fluid components. Heat structures are represented by one-dimensional or two-dimensional heat conduction in Cartesian or cylindrical coordinates. Temperature-dependent thermal conductivities and volumetric heat capacities can be provided in tabular or functional form either from built-in or user-supplied data. The modeling capabilities of heat structures can be used to predict the temperature distributions in solid components such as fuel pins or plates, heat exchanger tubes, and pipe and vessel walls, as well as to calculate the heat flux conditions for fluid components.

The thermal conduction inside the solid structures is governed by a diffusion equation:

$$\rho C_p \frac{\partial T}{\partial t} - \nabla(k \nabla T) - Q''' = 0 \tag{2}$$

Where k is the solid thermal conductivity, and Q''' is the volumetric internal heat source in the solid. It can be discretized in both Cartesian and cylindrical coordinates. The types of boundary conditions (BC) include: (1) Dirichlet BC, $T = T_0$; (2) Neumann BC, $k \nabla T = q_0''$; or (3) convective BC: $-k \nabla T = h \cdot (T - T_{fluid})$.

Since SAM is built on the MOOSE framework, it relies on the Jacobian Free Newton Krylov (JFNK) solution method to solve all the unknowns in a fully coupled fashion. This fully coupled solution scheme avoids the operator-splitting errors and is especially valuable for conjugate heat transfer problems in which the heat conduction in the solid is tightly coupled with the fluid flow. The JFNK method is a multi-level approach, using the outer Newton's iterations (nonlinear solver) and inner Krylov subspace methods (linear solver), to solve large nonlinear systems. The JFNK method has become an increasingly popular option for solving large nonlinear equation systems and multi-physics problems, as observed in a number of different disciplines [12].

In JFNK methods, the concept of 'Jacobian-free' is proposed, because deriving and assembling such large Jacobian matrices could be difficult and expensive. However, in most applications, the Krylov subspace methods require preconditioning to be efficient. This is especially true for the fluid flow and conjugate heat transfer problems. In the solution methods currently used in SAM, an approximate analytical Jacobian matrix is computed and passed to the underlying numerical solver library (PETSc) for preconditioning purposes.

3. CONJUGATE HEAT TRANSFER MODELING

3.1. Convective Heat Transfer at Fluid-Solid Interface

In many engineering applications, the fluid flow and solid heat conduction is coupled through convective heat transfer at the solid surfaces. The conjugated heat transfer modeling in SAM at the fluid-structure interface is shown schematically in Figure 1. The fluid is modeled as one-dimensional flow, and the solid structure is modeled as one-D or two-D heat conduction, and they exchange energy at the fluid-structure interface.

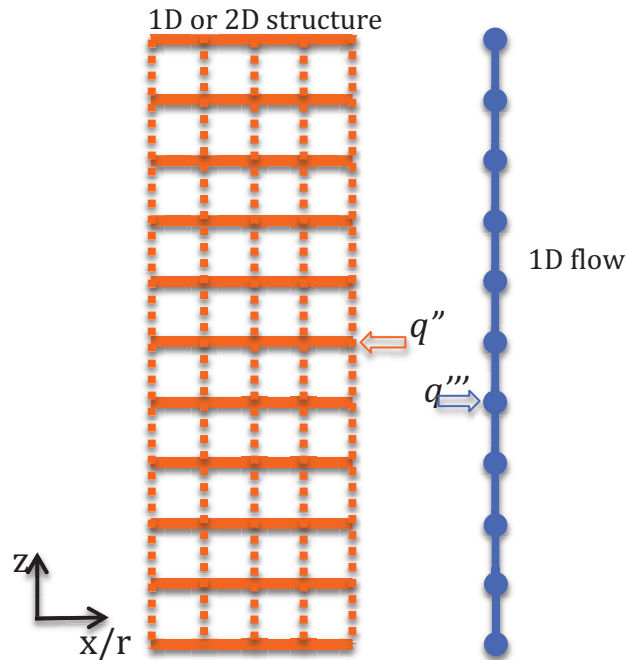


Figure 1: The Schematic of conjugate heat transfer modeling in SAM

At the fluid-structure interface, the convective heat flux is:

$$q'' = k\nabla T = h(T_w - T_f). \quad (3)$$

In which h is the heat transfer coefficient, T_w is the wall temperature, and T_f is the fluid temperature.

The weak form of the solid conduction equation (Eq.-2) can be written as,

$$\left(\rho C_p \frac{\partial T}{\partial t}, \psi \right) + (k\nabla T, \nabla \psi) - \langle k\nabla T, \psi \rangle - (Q''', \psi) = 0 \quad (4)$$

In which (f, ψ) represents the volume integral, $(f, \psi) = \int_{\Omega} \psi * f \, d\Omega$; and $\langle f, \psi \rangle$ represents the surface integral, $\langle f, \psi \rangle = \int_{\Gamma} \psi * f \, d\Gamma$. For one-D radial solid element at the interface, the convective heat flux can be directly applied as boundary conditions for the one-D heat conduction equation, as required by the $\langle k\nabla T, \psi \rangle$ term in Eq. (4).

However, for fluid element, it has to be modeled as an additional heat source term in the energy conservation equation,

$$q''' = h(T_w - T_f) \frac{P_{heated}}{A_c}. \quad (5)$$

This is implemented as an additional term in the residual calculation at each fluid node (quadrature point):

$$\Delta r_{energy} = JxW \cdot q''' \cdot \phi = JxW \cdot h(T_w - T_f) \frac{P_{heated}}{A_c} \cdot \phi, \quad (6)$$

In which, JxW is Jacobian times weight, and ϕ is the shape function. Eq. (6) is derived from the discretized form of $\int_{\Omega} \psi * q''' d\Omega$. Note the above implementation may introduce another term in the stabilized fluid model formulation. For the SUPG (Streamline Upwind Petrov-Galerkin) scheme used in SAM,

$$\Delta r_{energy} = JxW \cdot h(T_w - T_f) \frac{P_{heated}}{A_c} \cdot (\phi + \tau_{supg} \cdot \nabla \phi). \quad (7)$$

3.2. Preconditioning of Convective Heat Transfer Modeling

As mentioned above, a Krylov-type of method generally requires preconditioning to be efficient and effective. It is also well known that the closer the preconditioning matrix is to the exact Jacobian matrix, the better the convergence behavior. In SAM, an approximation of the exact Jacobian is provided to the solver as a preconditioning matrix, as the exact Jacobian matrix is very difficult to obtain and not necessary. For one-dimensional flow and heat conduction problems, tri-diagonal terms, due to spatial discretization, are included in the preconditioning matrix. Since the conjugate heat transfer is a tightly coupled phenomenon between the solid conduction and fluid flow, its Jacobian terms must be included.

The Jacobian terms represent the effect of one variable perturbation on the residuals of another variable. For convective heat transfer between fluid and structure, the Jacobian terms can be derived as:

$$\begin{aligned} J(T_s, T_s) &= \frac{\partial[h(T_w - T_f)]}{\partial T_f} \approx h \\ J(T_s, T_f) &= \frac{\partial[h(T_w - T_f)]}{\partial T_f} \approx -h \\ J(T_f, T_s) &= \frac{\partial[h(T_w - T_f) \frac{P_{heated}}{A_c}]}{\partial T_w} \approx -h \frac{P_{heated}}{A_c} \\ J(T_f, T_f) &= \frac{\partial[h(T_w - T_f) \frac{P_{heated}}{A_c}]}{\partial T_w} \approx h \frac{P_{heated}}{A_c} \end{aligned} \quad (8)$$

In which T_f and T_s represent fluid and solid temperature, respectively. Note in Eq. (8) that the dependences of heat transfer coefficient, h , on the fluid and solid variables are neglected.

For a conjugate heat transfer problem with only one fluid block and one solid block, the shape of the preconditioning matrix looks like Figure 2, in which the circles and red dots represent the non-zero entries from the convective heat transfer between fluid and structures. A similar study on the preconditioning of JFNK method for conjugate heat transfer problem can be found in [13].

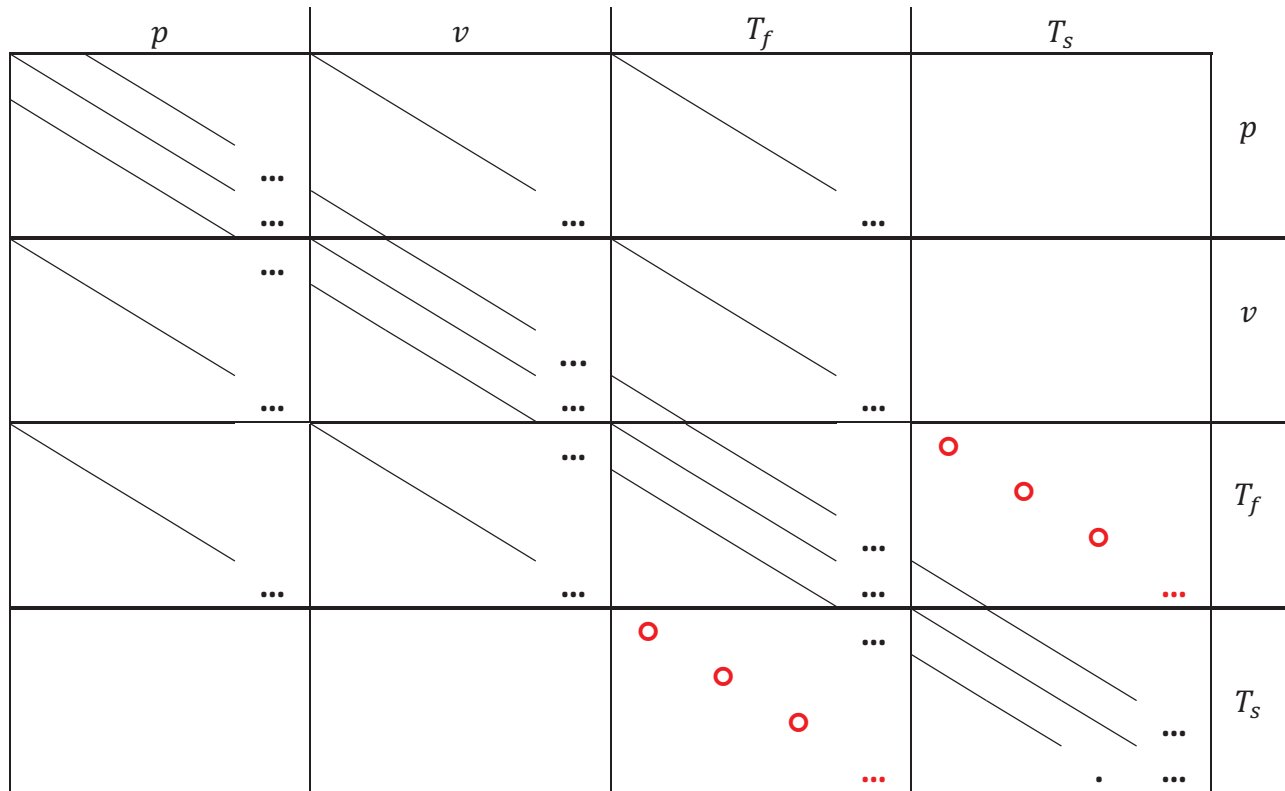


Figure 2: Preconditioning matrix for conjugate heat transfer problem (with lines, circles, and dots representing non-zero entries in the matrix)

4. DEMONSTRATION CALCULATION OF 7 FUEL ASSEMBLIES

4.1. Model Description

A 7-assembly model has been developed to examine the pseudo 3-D full-core conjugate heat transfer modeling capability in SAM. The fuel assembly geometry is based on the Advanced Burner Test Reactor (ABTR) conceptual design [1], and the major parameters of the ABTR fuel assembly design are listed in Table 1.

Table 1: ABTR Fuel Assembly Parameters

Assembly Parameters	
Pin number	217
Assembly pitch (m)	0.14598
Duct outside flat-to-flat distance (m)	0.14198
Duct inner flat-to-flat distance (m)	0.13598
Assembly duct thickness (m)	0.003
Inter-assembly gap width (m)	0.004
Assembly length (m)	0.8
Pin Parameters	
Pin diameter (m)	0.008
Pin pitch-to-diameter ratio	1.13
Pin pitch (m)	0.00904

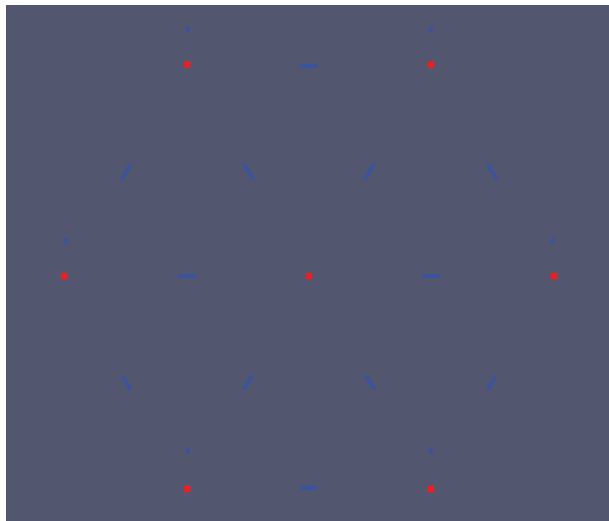
Seven identical fuel assemblies of 217 pins each are modeled in this study. The system T/H and the CFD models of this 7-assembly problem are shown in Figure 3. In the SAM model, it is modeled with seven 1-D parallel channels representing the subassembly flow, and 2-D structures representing the duct walls and the inter-assembly sodium gaps. Note that the 6 sides of the hexagon duct wall are modeled separately to account for different temperatures and heat transfer between inner assembly flow and each side of the duct wall. The red dots in Figure 3a represent the fluid nodes; the 12 blue lines between two fluid nodes represent all the heat structures between two assemblies (including two duct wall widths and the inter-assembly sodium gap); and 6 other blue lines near the fluid nodes represent the duct wall sides with adiabatic boundary conditions on the outside surface. For simplicity, the inter-assembly flow in the gap is neglected in this work, and only heat conduction is considered. A CFD model is also developed for comparison, as seen in Figure 3b. For simplicity (in the CFD simulation), only bare-bundle simulations were performed in this code-to-code benchmark exercise, and constant thermophysical properties of the sodium and duct wall are used in this work.

In the 7-assembly model, it is assumed that the center assembly (Channel 0) has higher power density with power peaking factor of 1.5, and that the lower-right assembly (Channel 6) has lower power density with power peaking factor of 0.5. All the other assemblies have the same power density with power peaking factor of 1. Uniform power distributions (both radial and axial) are assumed within each assembly. Additionally, the same inlet flow rate is applied for all assemblies.

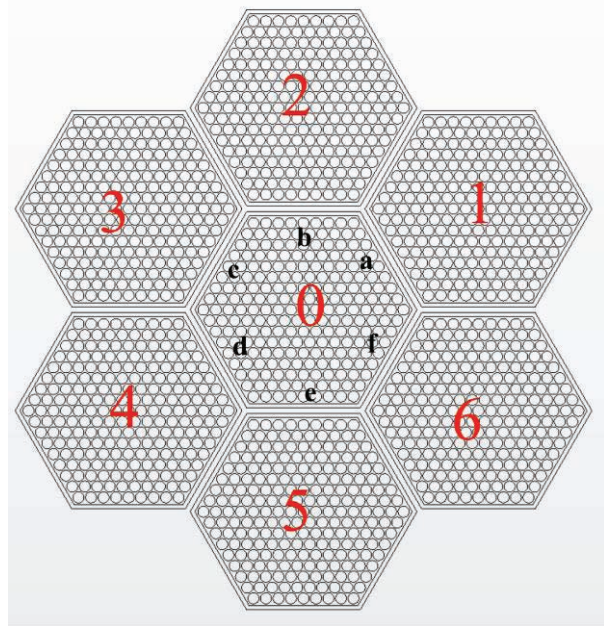
Name rule:

Number: assemble position (0~6)

Alphabet: wall position (a, b, c, d, e, f)



(a) System TH model

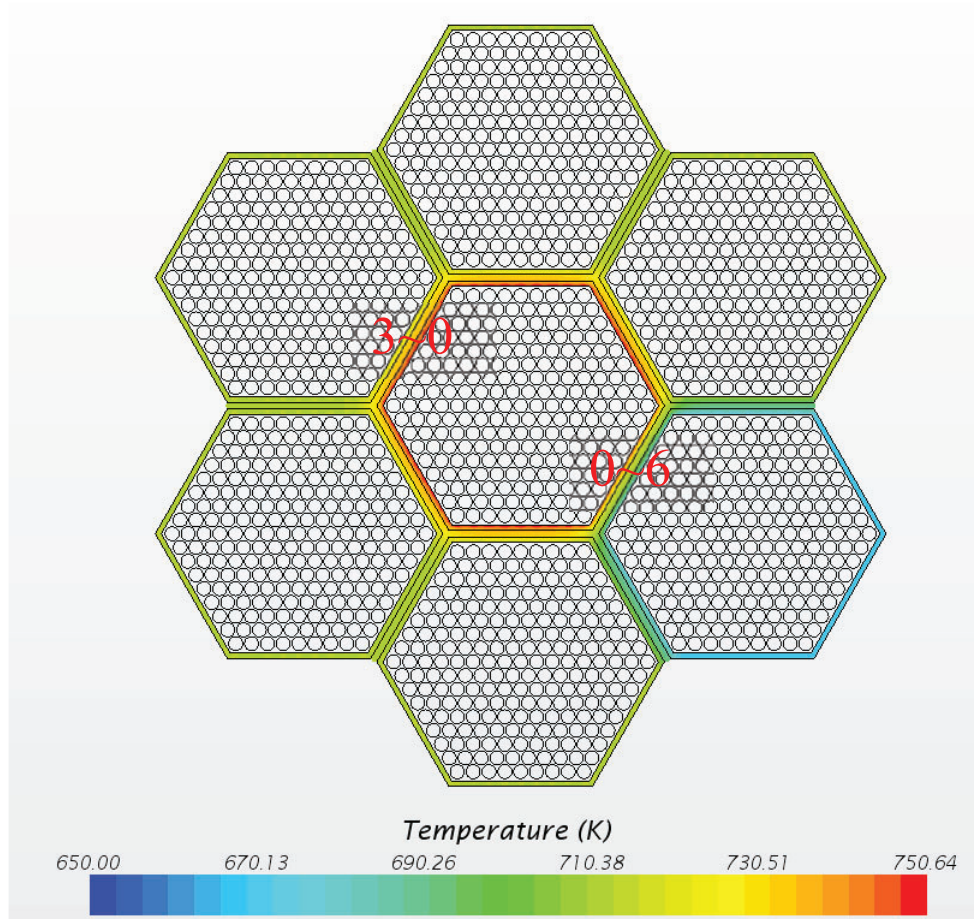


(b) CFD model

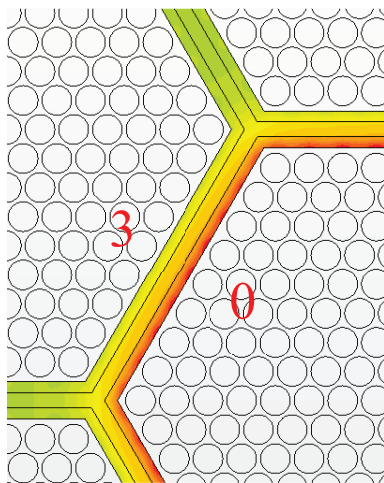
Figure 3: The 7-assembly computational model (top view) and notations

4.2. CFD Simulation Results

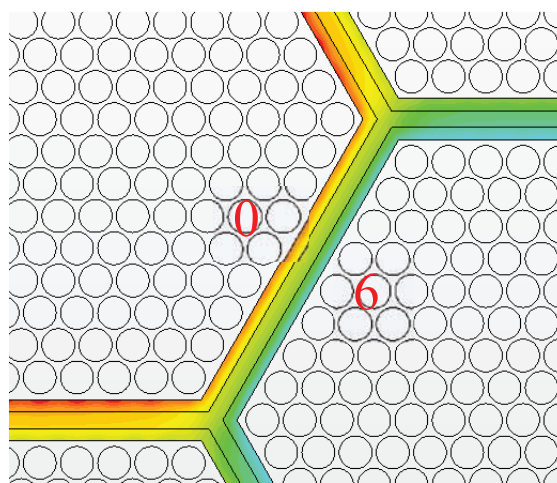
Realizable k- ϵ turbulence model, the two-layer all- y^+ wall formulation, and segregated flow solver with the SIMPLE predictor-corrector algorithm are used in the CFD simulation. The solution is well converged as the normalized residuals are below 10^{-4} . Figure 4 presents the temperature distributions at the core outlet of the 7-assembly CFD simulation. It is seen that the hot and cold assemblies significantly affected the duct wall temperatures of the neighbor assemblies. However, the effect diminishes with increasing distance from neighbor assembly ducts to these two assemblies.



(a) Duct walls and assembly gap temperature distribution



(b) Between assembly #0 and #6



(c) Between assembly #0 and #3

Figure 4: Duct wall temperature distributions at the core outlet of 7-assembly CFD simulation

4.3. Initial Comparison between CFD and SAM Results

The average axial temperature distributions from SAM and CFD simulations are compared in Figure 5. It is seen that the average coolant temperature predictions in the high power channel (Assembly 0) and low power channel (Assembly 6) agrees very well between the two approaches. However, large differences were observed for the duct wall temperatures. It is noted that inner temperature of Side C of Channel 6 duct wall is lower than the average coolant temperature in CFD simulation, while it is higher than the coolant temperature in the SAM simulation.

To better understand the differences between the two approaches, the coolant temperature distributions at the core outlet of Assembly 0 and 6 from the CFD simulation are shown in Figure 6. It is seen that the edge region of the two assemblies are much colder than the inner regions. Similar findings were also found in the authors' previous work on CFD simulations of wire-wrapped fuel assemblies. It is also confirmed that the temperature of duct wall 6C is higher than the coolant temperature near the wall in the CFD simulation; therefore, the coolant of Assembly 6 is actually receiving heat from the wall 6C, although its average coolant temperature is higher than the wall. However, in the SAM simulation above, only one average coolant temperature is modeled per assembly. Therefore, to correctly model the heat transfer direction between the assemblies, the duct wall temperature predictions are significantly overestimated in the SAM simulation.

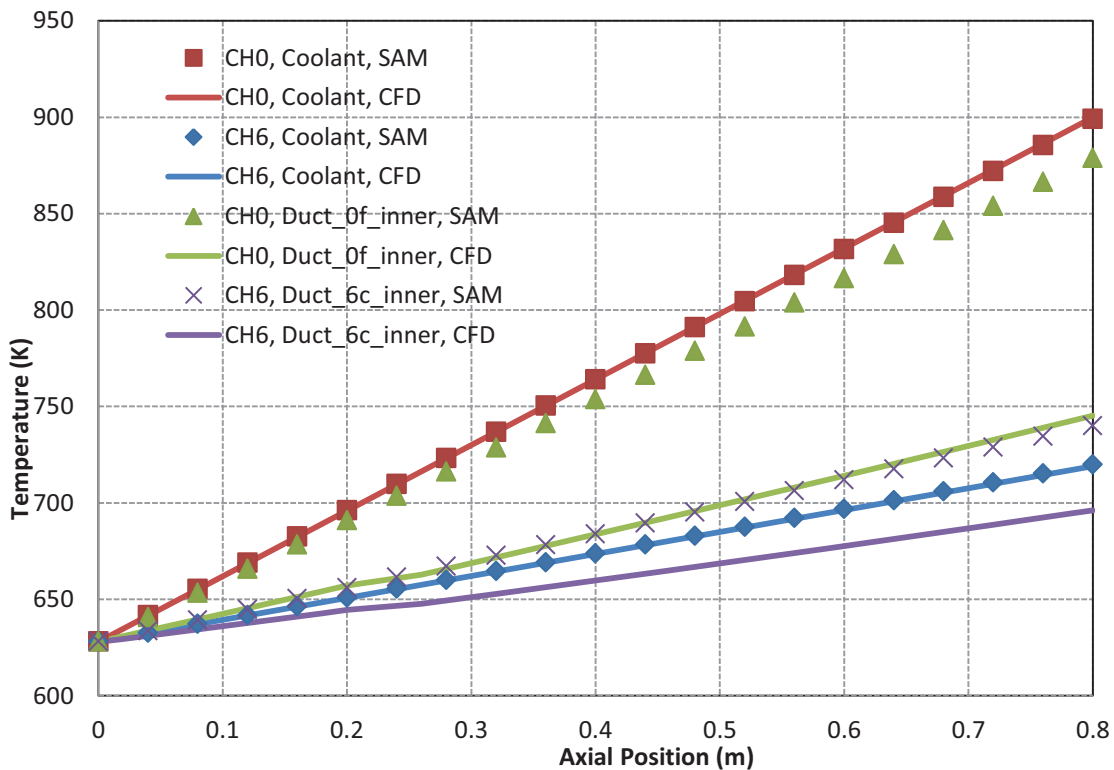


Figure 5: Comparison of average axial temperature distributions between SAM and CFD

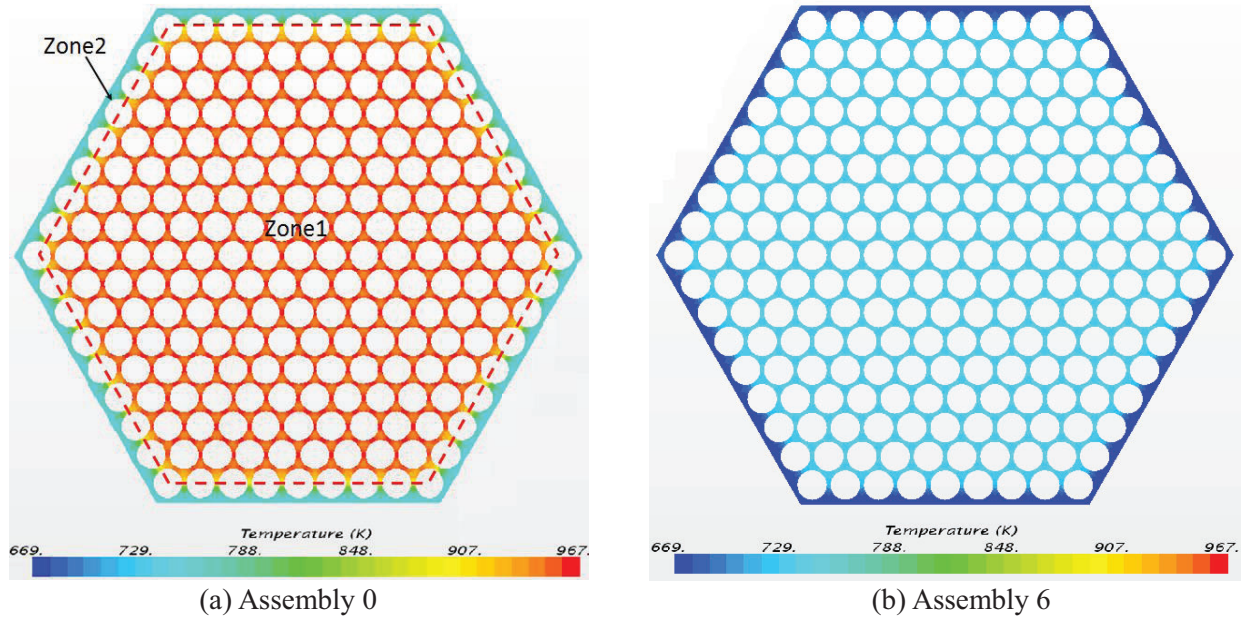


Figure 6: Coolant temperature distribution at core outlet of assembly 0 and 6

4.4. SAM Two-Region Core-Channel Model and Results

To improve the heat transfer between the duct wall and coolant flow, a two-region core channel model is developed in SAM to account for the temperature differences between the center region and the edge region of the coolant channel in a fuel assembly, as marked in Figure 6a. For a regular triangular lattice pin bundle, the flow area, heated and wetted perimeters, and the equivalent hydraulic and heated diameters of the two regions are well defined. In the SAM two-region model, the two fluid regions are modeled as two separate pipes with the same pressure drop and no net mass exchange. However, the heat exchange is possible at all axial nodes, and the energy exchange rate is modeled as:

$$\frac{d\dot{Q}}{dz} = \beta(\rho v)_{avg} S(h_1 - h_2) \quad (9)$$

in which, β is the mixing parameter (accounting for both turbulent mixing and directional flow); $(\rho v)_{avg}$ is the average mass flux between Region 1 and 2; S the total gap width between Region 1 and 2; and h_1 and h_2 are the enthalpies of Region 1 and 2.

Based on an energy balance calculation using the CFD simulation results, it is found that the energy exchange between the inner and edge zones is very small comparing to the heating power in each zone for the 7-assembly test problem. Therefore, $\beta = 0$ was assumed in the SAM analysis of this demonstration problem.

The axial temperature distributions of the Channel 0 and 6 from the SAM two-region model simulation are shown in Figure 7. Note that the temperature differences between the inner wall and the edge coolant are the same for Channel 0 and 6, indicating the convective heat transfer is balanced at the two sides of the inter-assembly heat structures. It is seen that the inner wall temperature of Duct 6C is lower than the average coolant temperature of Channel 6, but higher than the edge coolant temperature, as has been observed in the CFD simulation. In the two-region model, Zone 2 (edge region) has lower power density (for the total volume of pin and coolant regions), but higher mass flux (due to the larger hydraulic diameter and less friction coefficient). Therefore, its temperature would be much lower than that of Zone 1 (inner region). Since the duct wall would only interact with the edge zone, the wall temperature

predictions would be much lower comparing to those in the simulation using one-region model, as observed from Figure 5 and Figure 7.

The radial temperature distributions of the six sides of Channel 0 duct wall at the core outlet are shown in Figure 8. It is seen the temperature of Duct 0F is significantly lower than the other sides, as it faced the lower power Channel 6. The temperature differences among the other 5 sidewalls are negligible. This is because the inter-assembly heat transfer is very small compared to the heating power from the fuel rod, and the 5 average-power assemblies have almost the same coolant temperature predictions despite their positions relative to the high- or low-power assembly. For the center high-power assembly, the total heat removal between coolant and the six sides of the duct is ~ 22.5 kW, which is only $\sim 0.3\%$ of the heating power (7.58 MW).

The axial temperature distributions from the SAM 2-region model are compared with the average temperatures from the CFD simulation results, as shown in Figure 9. The radial wall temperature distributions of the heat structure between Channel 0 and Channel 6 at the core outlet are shown in Figure 10. Linear temperature distributions are observed in the Duct 0F, the inter-assembly sodium gap, and duct 6C in both SAM and STAR-CCM+ simulations. Very good agreements have been achieved between the two approaches. It can be concluded that the SAM 2-region model can accurately predict the duct wall temperatures in a 3-D core lattice layout. It should be noted that the SAM code is very efficient as it only takes less than ten seconds on a single processor for this demonstration simulation, while the CFD simulation takes ~ 20 hours on 128 processors.

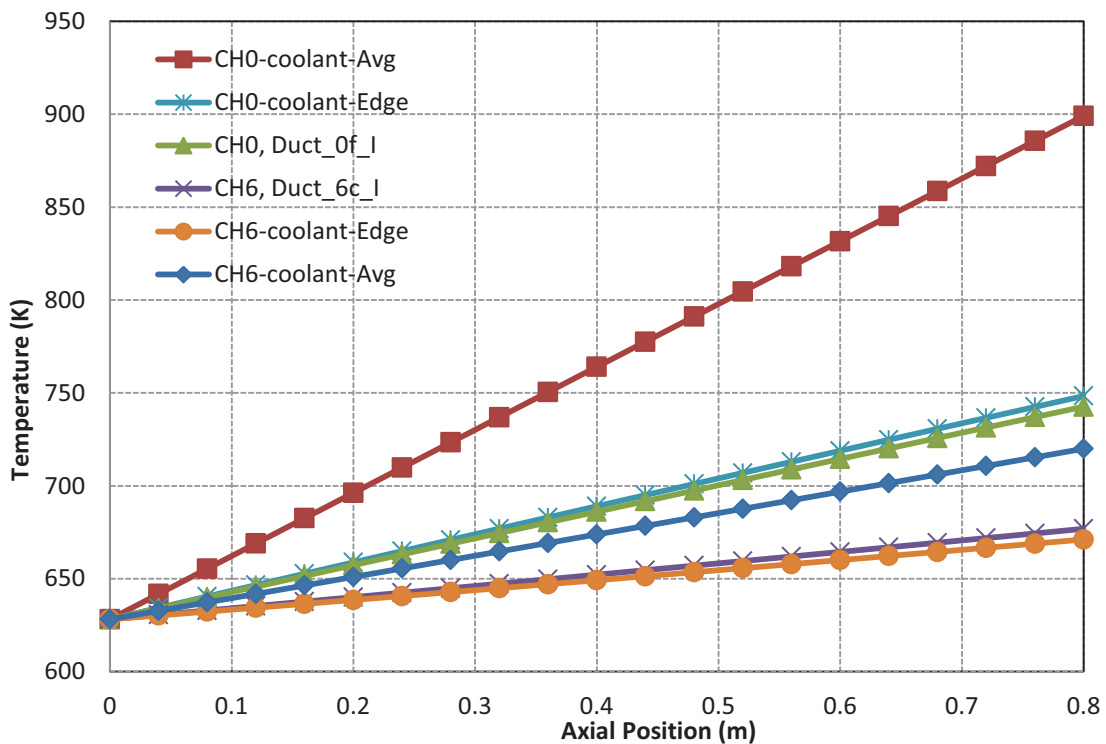


Figure 7: Axial temperature distributions of the Channel 0 and 6, SAM two-region model

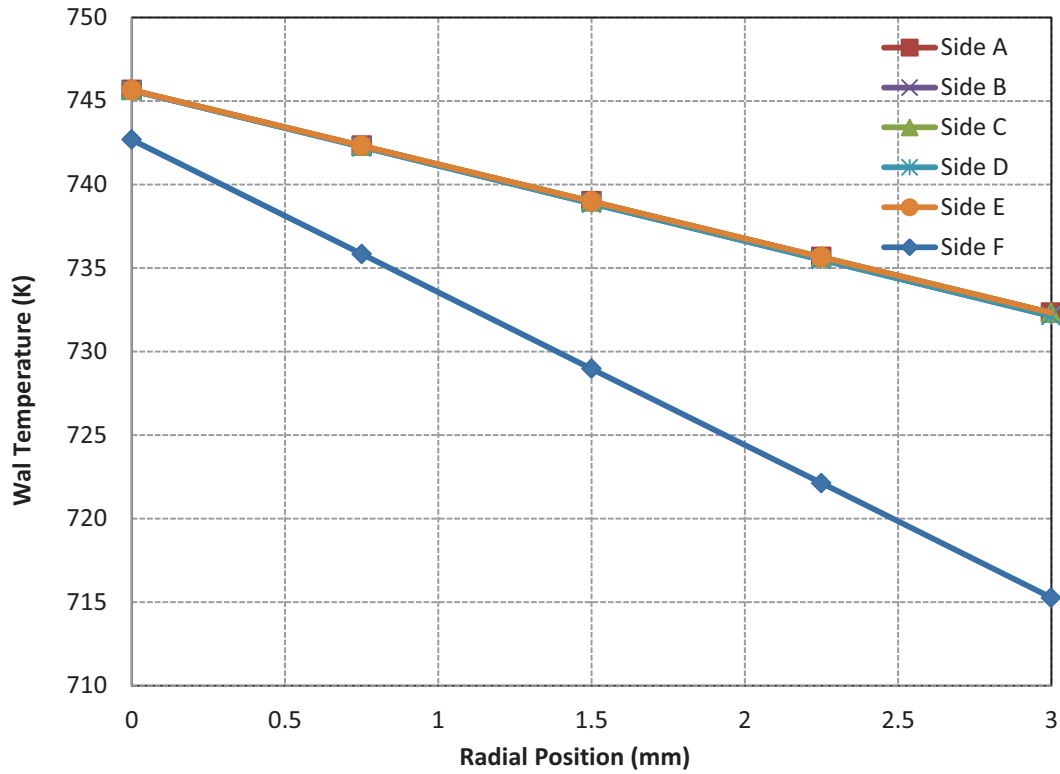


Figure 8: Radial temperature distributions of the six sides of Channel 0 duct wall, at the core outlet

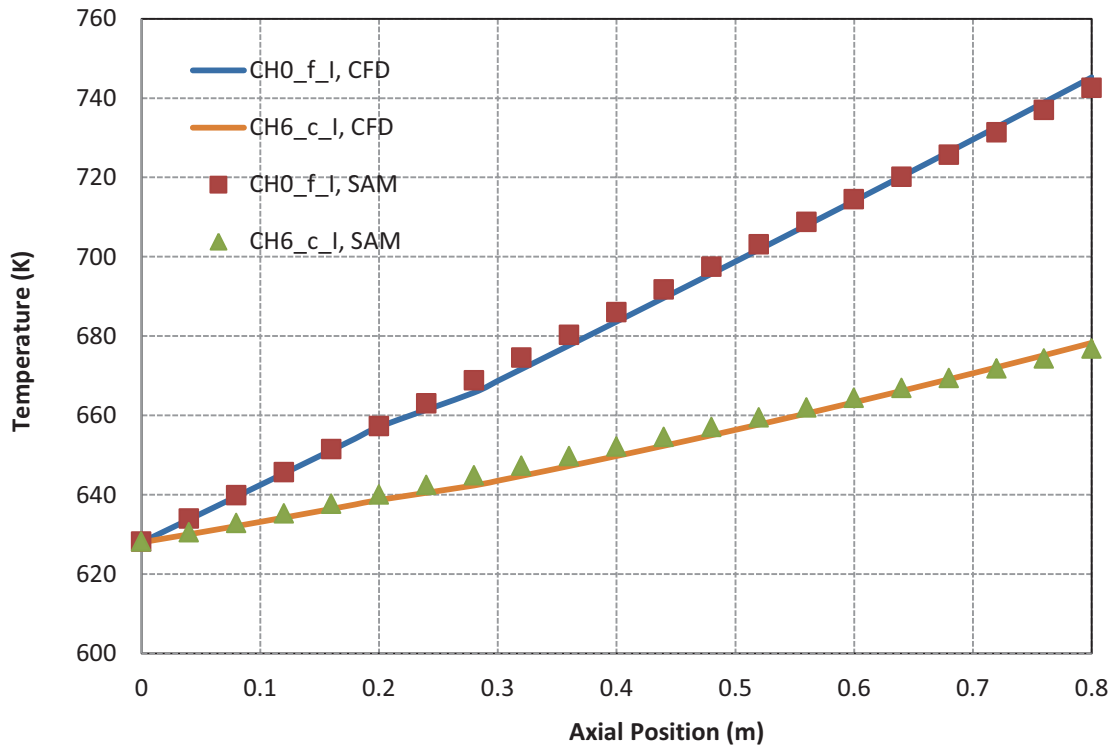


Figure 9: Comparison of average axial wall temperature distributions between SAM 2-region model and CFD

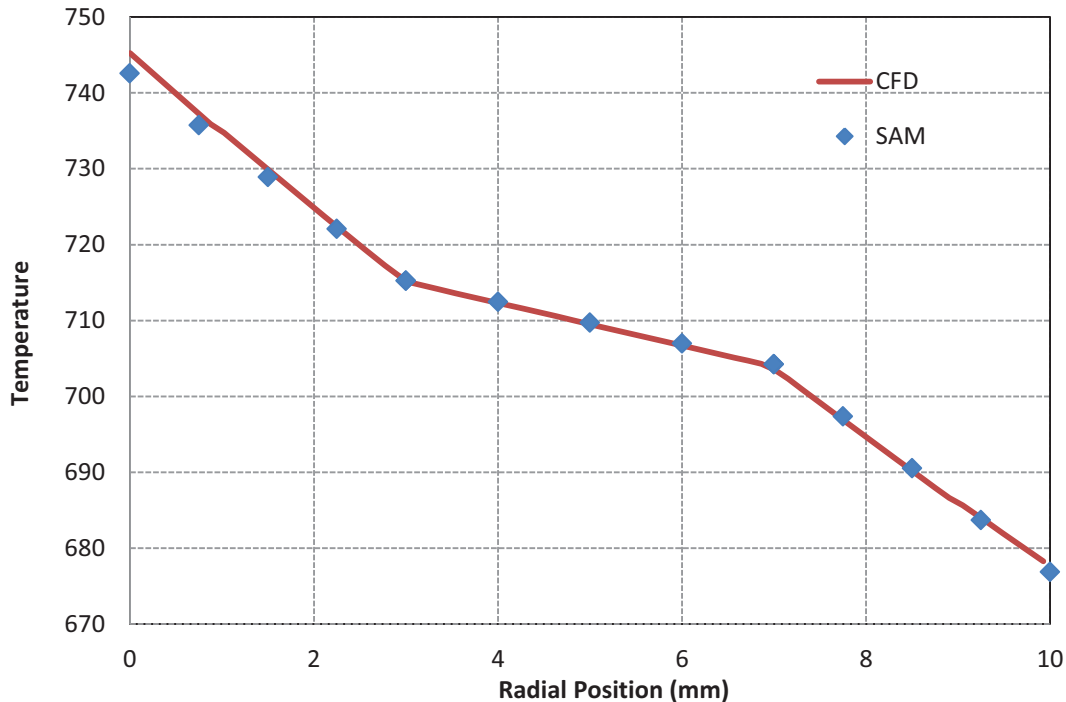


Figure 10: Comparison of radial wall temperature distributions between SAM 2-region model and CFD, heat structure between channel 0 and channel 6 at the core outlet

5. CONCLUSIONS

A pseudo 3-D full-core conjugate heat transfer modeling capability has been developed for the advanced system analysis tool SAM for efficient and accurate temperature predictions of SFR structures. The hexagon lattice core is modeled with 1-D parallel channels representing the subassembly flow, and 2-D duct walls and inter-assembly gaps. The six sides of the hexagon duct wall are modeled separately to account for different temperatures and heat transfer between inner assembly flow and each side of the duct wall. A core lattice model is developed to facilitate the generation of all the core channels and inter-assembly gaps. The Jacobian Free Newton Krylov (JFNK) solution method is applied to solve the fluid and solid field simultaneously to avoid the operator-splitting errors, which is especially valuable for conjugate heat transfer modeling.

The 3-D full-core conjugate heat transfer modeling capability in SAM has been demonstrated by a verification test problem with 7 fuel assemblies in a hexagon lattice layout. The simulation results are compared with RANS-based CFD simulations. It was found that a lumped coolant channel model (one temperature per axial position) would significantly overestimate the duct wall temperatures. Instead, a two-region core channel model is required to accurately model the duct wall temperature and inter-assembly heat transfer. Using the two-region model, SAM predictions agree very well with the results from the CFD simulation, while the computational cost is reduced by 6 orders of magnitude. It can be concluded that the SAM can efficiently and accurately model the inter-assembly heat transfer and the duct wall temperatures in a 3-D core lattice layout.

ACKNOWLEDGMENTS

This work is supported by U.S. DOE Office of Nuclear Energy's Nuclear Energy Advanced Modeling and Simulation (NEAMS) program. The submitted manuscript has been created by UChicago Argonne, LLC, Operator of Argonne National Laboratory ("Argonne"). Argonne, a U.S. Department of Energy Office of Science laboratory, is operated under Contract No. DE-AC02-06CH11357.

REFERENCES

1. Y. I. Chang, P. J. Finck, C. Grandy, et al., "Advanced Burner Test Reactor Preconceptual Design Report," ANL-ABR-1 (ANL-AFCI-173), Argonne National Laboratory, September 2006.
2. Y. Yu, E. Merzari, and J. Thomas, "SFR Duct Wall Temperature Prediction with a Porous Medium Model," *Transactions of the American Nuclear Society*, Vol. 111, 1651-1653, (2014).
3. D. Tenchine, "Some thermal hydraulic challenges in sodium cooled fast reactors," *Nuclear Engineering and Design*, 240, 1195-1217, (2010).
4. R. Hu and T. H. Fanning, "NEAMS SFR System Module: Overview and Development Status," *Proceedings of ICAPP 2014*, Charlotte, USA, April 6-9, 2014.
5. R. Hu, "An Advanced One-Dimensional Finite Element Model for Incompressible Thermally Expandable Flow", *Nuclear Technology*, Vol. 190, No. 3, 313-322, (2015).
6. R. Hu, "A High-Order System Thermal-Hydraulics Model for Advanced Reactor Safety Analyses," *Proceedings of NURETH-16*, Chicago IL, USA, August 30-September 3, 2015.
7. CD-adapco, "STAR-CCM+ v 9.04.009 User Manual," New York, 2014.
8. D. Gaston, C. Newman, G. Hansen, and D. Lebrun-Grandi'e, "MOOSE: A parallel computational framework for coupled systems of nonlinear equations," *Nuclear Engineering and Design*, vol. 239, pp. 1768-1778, (2009).
9. B. S. Kirk, J. W. Peterson, R. H. Stogner, and G. F. Carey, "libMesh: A C++ Library for Parallel Adaptive Mesh Refinement/Coarsening Simulations," *Engineering with Computers*, 22(3-4): 237-254, (2006).
10. S. Balay, J. Brown, et al, PETSc Web page, <http://www.mcs.anl.gov/petsc>, 2015.
11. R. Hu and T.H. Fanning, "Update on Developments for the SFR System Analysis Module," ANL/NE-14/9, Argonne National Laboratory, September 2014.
12. D. A. Knoll and D. E. Keyes, "Jacobian-free Newton-Krylov Methods: a Survey of Approaches and Applications," *Journal of Computational Physics*, Vol. 193, pp.357-397 (2004).
13. L. Zou, J. Peterson, H. Zhao, et al., "Solving Implicit Multi-Mesh Flow and Conjugate Heat Transfer Problems with RELAP-7," *Proceedings of M&C 2013*, Sun Valley, Idaho, May 5-9, 2013.